

Alma Mater Studiorum Università di Bologna
Archivio istituzionale della ricerca

Respiratory Activity Monitoring by a Wearable 5.8 GHz SILO With Energy Harvesting Capabilities

This is the final peer-reviewed author's accepted manuscript (postprint) of the following publication:

Published Version:

Paolini G., Al Shanawani M., Masotti D., Schreurs D.M.M., Costanzo A. (2021). Respiratory Activity Monitoring by a Wearable 5.8 GHz SILO With Energy Harvesting Capabilities. IEEE JOURNAL OF ELECTROMAGNETICS, RF AND MICROWAVES IN MEDICINE AND BIOLOGY., 6(2), 246-252 [10.1109/JERM.2021.3132201].

Availability:

This version is available at: <https://hdl.handle.net/11585/844135> since: 2022-05-25

Published:

DOI: <http://doi.org/10.1109/JERM.2021.3132201>

Terms of use:

Some rights reserved. The terms and conditions for the reuse of this version of the manuscript are specified in the publishing policy. For all terms of use and more information see the publisher's website.

This item was downloaded from IRIS Università di Bologna (<https://cris.unibo.it/>).
When citing, please refer to the published version.

(Article begins on next page)

This is the final peer-reviewed accepted manuscript of:

G. Paolini, M. Shanawani, D. Masotti, D. M. M. . -P. Schreurs and A. Costanzo, "Respiratory Activity Monitoring by a Wearable 5.8 GHz SILO With Energy Harvesting Capabilities," in *IEEE Journal of Electromagnetics, RF and Microwaves in Medicine and Biology*, vol. 6, no. 2, pp. 246-252, June 2022

The final published version is available online at:

<https://doi.org/10.1109/JERM.2021.3132201>

Terms of use:

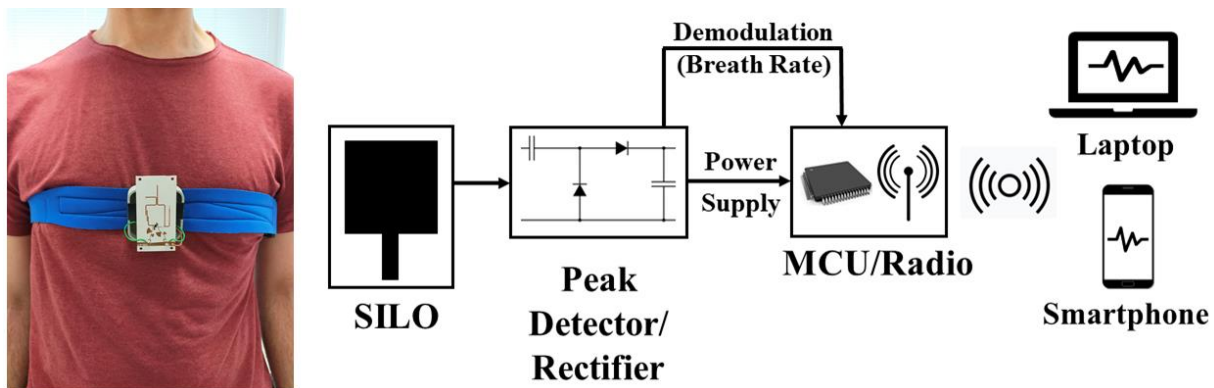
Some rights reserved. The terms and conditions for the reuse of this version of the manuscript are specified in the publishing policy. For all terms of use and more information see the publisher's website.

This item was downloaded from IRIS Università di Bologna (<https://cris.unibo.it/>)

When citing, please refer to the published version.

Respiratory Activity Monitoring by a Wearable 5.8 GHz SILO with Energy Harvesting Capabilities

Giacomo Paolini, *Member, IEEE*, Mazen Shanawani,
Diego Masotti, *Senior Member, IEEE*, Dominique Schreurs, *Fellow, IEEE*,
and Alessandra Costanzo, *Senior Member, IEEE*



Envisioned scenario for the wearable sensor aiming at normal and deep breath rate detection, working at 5.8 GHz, and able to harvest energy for feeding a commercial microcontroller unit.

Take-Home Messages

- This work describes the design and the realization of a wearable sensor working at 5.8 GHz exploiting the self-injection locking radar technique for human breath detection.
- The sensor allows detecting inhalations and exhalations of monitored subjects living their normal life, as well as deep and fast breath that could reveal dangerous situations. The device is of reduced dimensions, fully wearable, and is located at a certain distance from the user's body at the chest position.
- The sensor architecture is conceived in such a way that it does not need a dedicated receiving station to be placed in the surrounding environment (such as a spectrum analyzer), since an FM-to-AM demodulator is embedded into the sensor itself, with the possibility to work without the need of any anchor nodes nor remotely synchronized receivers.
- As a distinctive peculiarity with respect to the already existing solutions, the demodulator can further be exploited as an RF-to-DC rectifier for energy harvesting purposes. The harvested energy can be used, for instance, to supply an ultra-low-power microcontroller equipped with a transceiver in order to send wirelessly breath rate data to a laptop or a smartphone.
- Data processing of the rectifier/demodulator output is thus enabled on board with the goal of raising an alarm wirelessly only whenever a dangerous situation is detected (i.e., in presence of hyperventilation). In this way, the power-hungry transmitter operations are minimized with respect to continuous transmission of the breath rate data.

Respiratory Activity Monitoring by a Wearable 5.8 GHz SILO with Energy Harvesting Capabilities

Giacomo Paolini, *Member, IEEE*, Mazen Shanawani,
Diego Masotti, *Senior Member, IEEE*, Dominique Schreurs, *Fellow, IEEE*,
and Alessandra Costanzo, *Senior Member, IEEE*

Abstract — In this work, the design and the realization of a pocket-size sensor for breath rate detection are presented. Exploiting the self-injection locking radar technique, it is possible to perform FM-to-AM demodulation that allows the detection of the voltage peaks at the output of the sensor's receiving part. If compared with existing solutions, this device is of reduced dimensions and fully wearable; in fact, it can be worn by the user at a certain distance from the body at the chest position, and work without the need of any dedicated remotely synchronized anchor nodes nor bulky analyzers to be carried close by. As a more distinctive peculiarity, the receiving circuit is designed as an RF-to-DC rectifier in order to also enable the possibility to harvest energy that can be exploited, for instance, to feed a microcontroller unit and a transceiver with the aim of sending wirelessly the breath rate data to a laptop or a smartphone. Circuit simulations are corroborated by measurements in order to ensure the feasibility of the proposed solution.

Keywords — breath, demodulation, energy harvesting, microwaves, radar, self-injection, wearable.

I. INTRODUCTION

OVER these last years, the increasing attention towards wireless technologies for biomedical applications has led to the development of new devices and systems capable of assisting people in their daily living environments.

Specifically, several internet of things (IoT) applications are nowadays on the cutting edge because of their interoperability, ease of use, easy availability, and low cost; we can therefore talk about smart homes, smart cities, and smart health, among others. All these solutions are made possible by interconnecting intelligent objects exploiting the recent advances in wireless sensor networks (WSN), radiofrequency identification (RFID), artificial intelligence (AI), augmented reality, and so on.

Focusing on smart health (or e-health) applications [1], the adoption of a consistent network of sensors able to continuously monitor and transmit vital data to healthcare controllers [2], has resulted in the creation of the so-called wireless body area networks (WBAN). In particular, the correct detection of human vital signs, e.g., heart rate [3]-[6], fetal cardiac activity [7], [8], and especially breath rate

[4]-[6], [9], [10], is becoming more and more crucial in these last times, also considering the capability of early diagnosis of illnesses that could require hospitalization.

As an example, SARS-CoV-2 (severe acute respiratory syndrome coronavirus 2, or COVID-19) is an infectious disease caused by the most recently discovered coronavirus, that can gradually cause shortness of breath, limited respiratory function, and in some cases severe pneumonia [11]. One of the first signs of this condition can be traced in the accurate monitoring of an increasing resting breath rate [12]. If detected in time, this sign could lead to the identification of the disease in an early phase and therefore enable the possibility for the patient to get treatment in time before being forced to hospitalization.

When monitoring human vital signs such as breathing and heartbeat [13], the displacement to be detected is below centimeter level. For instance, considering the application of breath monitoring in adults, the peak-to-peak chest motion due to respiration, ranges from 4 to 12 mm [14], whereas normal breath rate ranges from 0.1 to 0.8 Hz.

In recent times, several works presented smart devices exploiting various radar approaches to detect the movement of the body under the effect of breath, by making use of frequency modulated continuous wave (FMCW) [15], ultrawideband (UWB) [16], and self-injection locked (SIL) [17]-[22] radar technique. The latter has been proved to be a good candidate, especially for breath rate detection, due to its high signal-to-noise ratio (SNR), high immunity to interferences, and low energy consumption. However, these devices are not stand-alone sensors because they require devoted external instrumentation, which can be in some

Manuscript submitted June 21, 2021.

G. Paolini, M. Shanawani, D. Masotti, and A. Costanzo are with DEI "Guglielmo Marconi", University of Bologna, Bologna 40136, Italy (e-mail: giacomo.paolini4@unibo.it, mazen.shanawani@unibo.it, diego.masotti@unibo.it, alessandra.costanzo@unibo.it).

G. Paolini and A. Costanzo are also with DEI "Guglielmo Marconi", University of Bologna, Cesena 47522, Italy.

D. Schreurs is with ESAT-Wavecore, KU Leuven, Leuven 3001, Belgium (e-mail: dominique.schreurs@kuleuven.be).

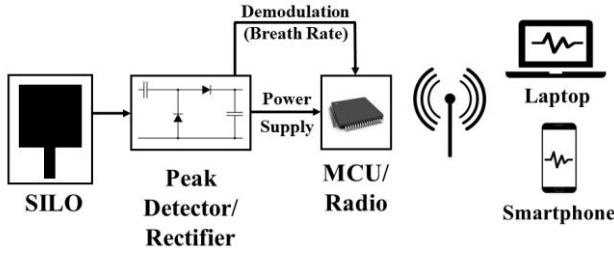


Fig. 1. An envisioned scenario of the wearable sensor for breath rate detection working at 5.8 GHz, able to detect human breath rate and to harvest energy for feeding a commercial SoC.

cases heavy, expensive, and not available to everyone, differently from a smartphone or a laptop. For these reasons, this work describes the design and the validation measurements of a fully wearable 5.8 GHz self-injection locked oscillator (SILO) sensor, in order to achieve a solution for human breath monitoring, by implementing and blending the ideas presented in [23] and [24].

Moreover, a smart solution for the receiving sub-system is proposed, exploiting a quarter-wavelength microstrip coupler linked with the SILO output port and connected to a passive demodulator/rectifying circuit. In this way, signal processing can be carried out in real-time and on-board. As an additional novelty, this subsystem is also able to provide the overall energy requirements of a system-on-a-chip (SoC) embedding microcontroller unit (MCU) and transceiver; the aim is to send breath rate data to the surrounding devices, as represented in the envisioned scenario of Fig. 1.

II. DESIGN METHOD

A. Self-Injection Locked Oscillator at 5.8 GHz

The radiating element of the 5.8 GHz sensor is a dual-port, dual-polarized, aperture-coupled patch antenna connected to the input and output ports of the SILO circuit (Fig. 2 (a)): the dielectric substrate for the patch antenna is Neltec NY9208, which is a typical substrate for antennas selected for its dielectric constant ($\epsilon_r=2.08$), thickness (1.524 mm), and low losses ($\tan(\delta)=0.0011$).

The ground plane is interposed between the antenna dielectric substrate and the Taconic RF60-A ($\epsilon_r=6.15$, thickness: 0.635 mm), i.e., the substrate of the feeding circuitry placed in the bottom layer. This substrate has been chosen in order to minimize the width (0.9 mm) of the 50- Ω feeding microstrip lines.

Moreover, the ground plane presents two orthogonal non-resonating slots allowing the electromagnetic (EM) coupling between the microstrip lines and the dual-polarized patch and, consequently, the feeding of the antenna itself. The microstrip feeding lines and the slots are positioned in such a way that the sensor can ensure two orthogonal linear polarizations at the input and output oscillator ports, as required by the SILO operating principles: through the output port (horizontally polarized), the RF signal at 5.8 GHz is transmitted in the direction of

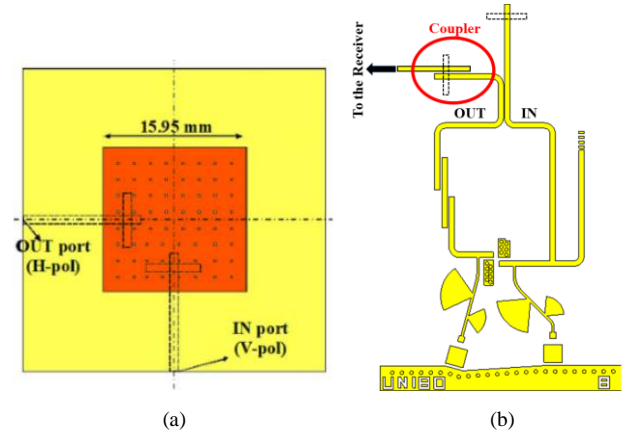


Fig. 2. (a) Front and (b) bottom view of the self-injection-locked oscillator, also with the quarter-wavelength microstrip coupler to be connected to the sensor receiving part. The slots etched in the ground plane for coupling IN and OUT microstrip lines with the patch are dashed for both sides. [24] © IEEE 2020

the chest of the subject under test, whereas through the input port (vertically polarized), the oscillator gets into a SIL state by receiving the signal reflected by the user's body, which is amplitude, phase, and frequency-modulated.

The holes in the patch metallization (see Fig. 2 (a)) guarantee isolation around 20 dB between the two ports. This was done to decouple the signal coming from the oscillator and the one backscattered by the subject's chest. It has been also verified that the power of the latter is higher for the vertical polarization (input) than the horizontal one (output), meaning that the reflection causes a change in the polarization of the signal [25].

In order to bias the pseudomorphic high electron mobility transistor (PHEMT) of the oscillator circuit, a battery and a voltage regulator have been used to provide the appropriate drain and gate voltages, $V_D=3.7$ V and $V_G=0.6$ V, respectively. This choice has been derived by the oscillator stability analysis [26] providing a stable build-up of the RF oscillation. An RF output power of about 10 dBm is achieved at the oscillator output port, with an overall PHEMT power consumption of 220 mW. Being the transmitted power equal to 10 dBm and the antenna gain to 6.84 dBi (versus 4.8 dBi in [27]), the corresponding effective isotropic radiated power (EIRP) value is equal to 16.84 dBm (~ 48 mW) for the present prototype.

With the aim of evaluating the effects of the SILO antenna body proximity, specific absorption rate (SAR) has been evaluated, referring to the limits established by the corresponding European and American regulatory bodies. The SAR value was mediated on a 10-g multi-layered volume of biological tissues (skin, fat, and muscle) by means of the simulation software CST Microwave Studio. The maximum SAR value averaged on a 10-g tissue volume was 0.44 W/kg for an antenna-chest distance of 2.5 cm. Therefore, this value resulted to be below the allowed limit of 2.00 W/kg, as established by the International Commission on Non-Ionizing Radiation Protection (ICNIRP).

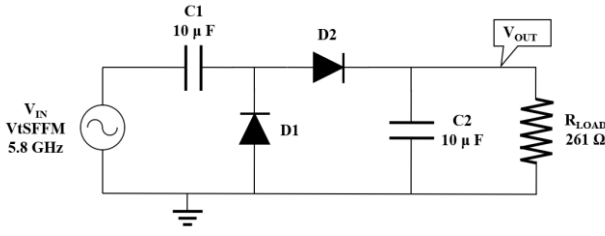


Fig. 3. Circuit schematic of the receiver sub-system coupled with the oscillator output (single frequency, frequency-modulated voltage source), acting as an FM demodulator and at the same time as an RF-to-DC converter for energy harvesting purposes.

B. Design of the Receiving Sub-System for Demodulation and Energy Harvesting

Once the SILO has transmitted the EM wave, the reflected one is phase, frequency, and amplitude-modulated by the chest movements; thus, the baseband signal can be acquired by frequency or amplitude demodulation techniques.

In [22], a similar system is proposed, where the SILO and the frequency demodulation are realized by means of integration and derivation sub-circuits. Indeed, the first-order differentiator straightforwardly allows to derive the time variations of the biomedical signal. The differentiator output is then connected to an active peak detector and a baseband amplifier.

Conversely, in the design presented in this work, the demodulation procedure is carried out by adopting a fully passive signal detector, which can at the same time act as a RF-to-DC rectifier to harvest part of the incoming power.

To the authors' knowledge, this solution has not been proposed before, i.e., a unique device able to harvest RF energy from the modulated tone at 5.8 GHz, while it is down-converted in order to retrieve the respiratory rate of the subject from the injected frequency variation.

In this proof-of-concept prototype, the oscillator is connected to the proposed rectifying/demodulator sub-system by means of a quarter-wavelength microstrip coupler, as described after in Section III.C.

Its circuit schematic is depicted in Fig. 3 and consists of a typical architecture of a voltage-doubler rectifier using two Schottky diodes (Skyworks SMS7630-079LF), two 10 μ F Murata RF capacitors, and a resistor ($R_{LOAD}=261 \Omega$), acting as the DC-load.

The capacitors and the load resistance have been optimized to simultaneously maximize the circuit performance from the point of view of FM-to-AM demodulation and RF-to-DC power conversion efficiency (PCE).

The receiver sub-system of Fig. 3 has been analyzed over time, using the Keysight ADS transient simulator, under the following operating conditions:

- excitation: frequency-modulated RF sinusoidal voltage source.
- Carrier frequency: 5.8 GHz.
- Input power (oscillator output power): 10 dBm.
- Modulating signal frequency (breath rate): 1 Hz.

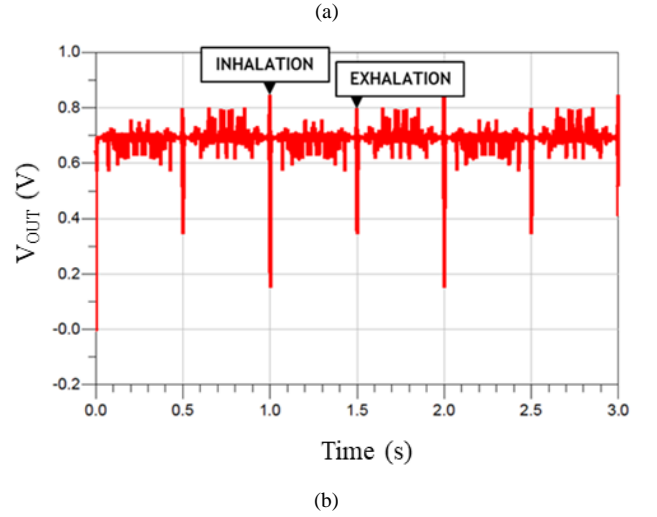
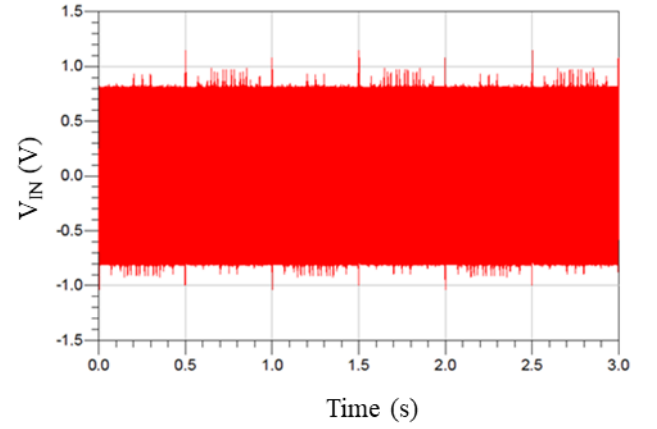


Fig. 4. Voltage waveforms of (a) the input FM signal with a carrier of 5.8 GHz and a modulating signal of 1 Hz, and (b) baseband signal at the output of the voltage-doubler rectifier.

- Maximum deviation of the instantaneous frequency: 10 MHz.
- Modulation index: $h=10^4$.
- Simulation time duration: 3 s.
- Maximum time step: 1 μ s.

The voltage source V_{IN} is plotted in Fig. 4 (a) versus time. It emulates the signal generated by the oscillator, backscattered by the chest, and then locking the SILO. The peaks at the rectifier output are plotted in Fig. 4 (b): their detection occurs every second, corresponding to a 1-Hz modulation frequency emulating realistic tachypnea in adult subjects (typical values are in the range of 30-60 breaths/minute).

III. EXPERIMENTAL RESULTS

In this section, the experimental validation of the proposed system in both a controlled environment and with the system installed on-body is presented.

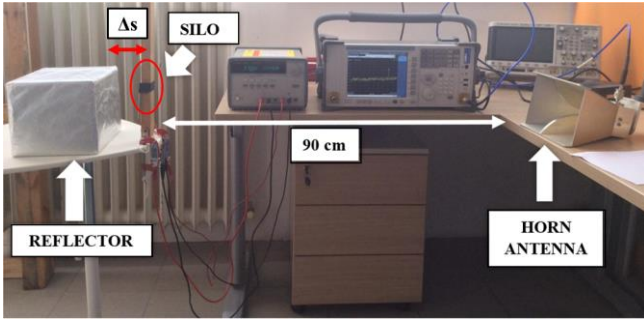


Fig. 5. Setup of the validation measurement enabling the frequency-modulation of the signal with the presence of a reflective object in front of the oscillator antenna.

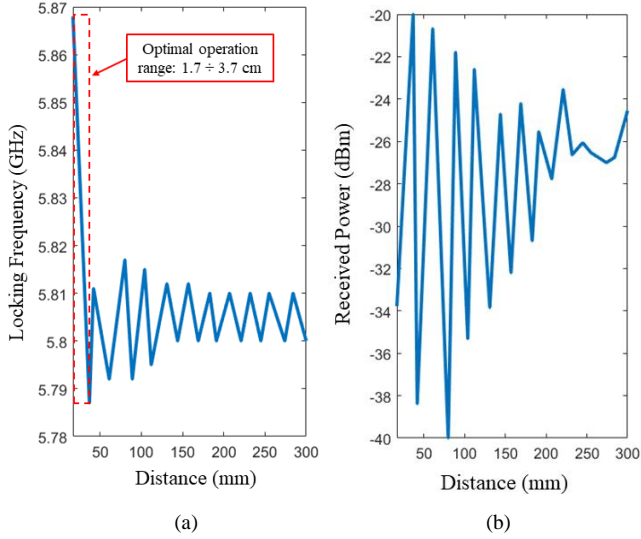


Fig. 6. (a) Locking frequency and (b) power received from the horn during displacement measurements of the oscillator antenna from a metallic reflector, for distances Δs ranging from 16 to 300 mm.

A. Measurements of the SIL Radar Performance in the Presence of a Metallic Reflector Located at Controlled Distances

First, to obtain a quantitative analysis of the SILO sensor, a metallic reflecting object mimicking the human body is moved away from the SILO antenna for variable controlled displacements up to a maximum distance of 30 cm (see the measurement setup of Fig. 5); with this method, it is possible to establish the minimum and maximum injection frequency for an engagement interval, with respect to the distance of the metallic reflector from the sensor.

These tests have been carried out several times and repeatable results have been collected through a remote receiving TDK HRN-0118 horn antenna connected to a spectrum analyzer (Fig. 5). Depending on the reflector-sensor distance (Δs), the following behavior has been observed:

- 1) when the reflector is located in the proximity of the SILO (between 0.1 mm and 13 mm), the received signal strength varies significantly; moreover, it

disappears when $\Delta s=13$ mm, approximately



Fig. 7. Photo of the SIL sensor placed at the user's chest for the first set of measurements.

corresponding to $\lambda/4$ at 5.8 GHz.

- 2) Increasing Δs , no injection locking takes place up to $\Delta s=16$ mm, where a 5.868 GHz locking frequency is observed again.
- 3) The largest locking range (80 MHz) is observed when $\Delta s=20$ mm. In these optimum conditions, a $\Delta f/\Delta s$ resolution of about 4 MHz/mm is achieved.
- 4) For higher reflector-SILO distances, a gradual reduction of the locking range is observed, but even for $\Delta s=30$ cm a locking range of 10 MHz is guaranteed.

These results are summarized in Figs. 6 where the measured locking frequency (Fig. 6 (a)) and the detected signal strength (Fig. 6 (b)) are plotted versus the reflector-sensor distance (Δs).

B. On-Body Breath Tests

This measurement campaign has been dedicated to the characterization of the SILO in more realistic operating conditions; its behavior has been tested on four different subjects wearing the sensor enclosed in a plastic case in order to ensure a distance of about 2.5 cm between their chest and the antenna. The case is held by a stretch band covering the trunk of the subject, as depicted in Fig. 7.

The locking frequency variations due to breathing activity are recorded, while the individuals stand in front of the horn antenna connected to a spectrum analyzer (again used as the receiving section of the system). A broadband antenna (at least 200-MHz-bandwidth, i.e., about 3.5% of relative bandwidth) allows complying with significant fluctuations of the locking frequency with respect to the individual chest's displacements. Redundant information is collected by performing the measurements for three horn-subjects distances, namely 1, 1.5, and 2 meters.

Some representative results of these on-body tests are

reported in Figs. 8, where the received power is plotted versus the SILO locking frequency (“maximum hold” mode

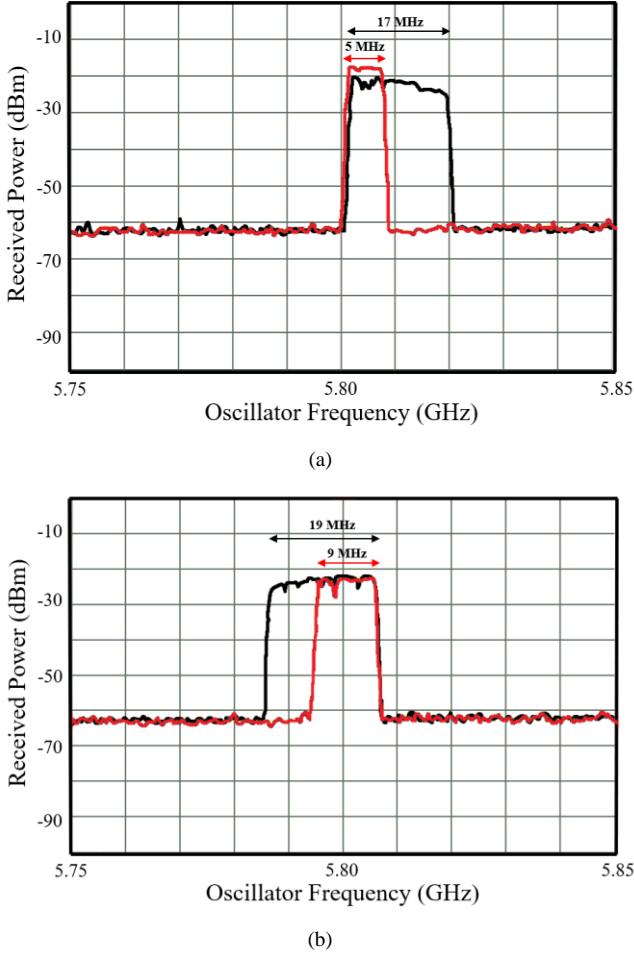


Fig. 8. The plots refer to measurements obtained for two subjects: (a) male subject with receiver placed at a distance of 1 meter; (b) female subject with receiver placed at 1.5 m. The red lines represent normal breath, whereas the black ones correspond to deep breath performed for 30 seconds.

of the spectrum analyzer has been used), confirming that, during respiration, the SILO input signal is frequency-modulated by the chest displacements. In practice, human breath acts as a frequency modulator and generates a frequency-shift-keying (FSK) signal whose deviation is proportional to the displacement of the chest with respect to the sensor’s antenna. The plots are shown for two different individuals wearing the same sensor but located at different distances from the receiver (this distance only affects the signal strength). During inspiration/expiration, it is possible to notice an increase/decrease of the oscillator locking frequency, with the largest locking frequency corresponding to the deepest breaths exercised by the subjects under test. Comparing the two plots, it can be noticed that, although the locking ranges are well distinguishable for normal and deep breaths, the effective locking frequency bandwidths and the respective central frequencies are individual-dependent.

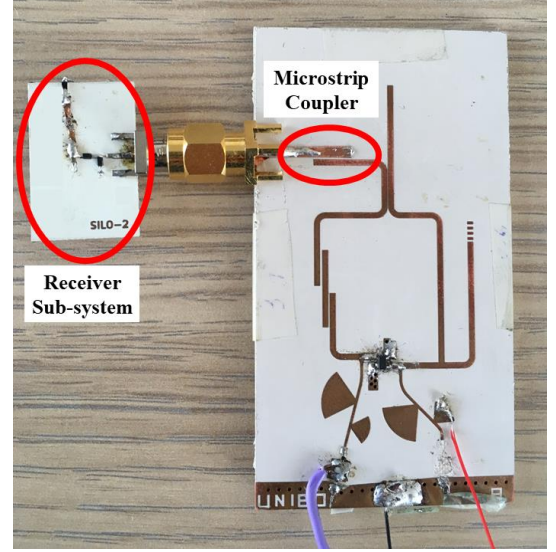


Fig. 9. Photograph of the breath sensor prototype, showing the connection of the oscillator output port to the receiving sub-system by means of a microstrip coupled line.

C. Receiver Demodulating Sub-System for FM-to-AM Conversion and Energy Harvesting Operations

With the aim of simplifying the system exploitation and getting rid of a remote receiving system (i.e., the broadband antenna connected to the spectrum analyzer), the microstrip line at the output port of the SILO has been coupled to the on-board FM demodulator presented in Section II.B.

The prototype and the connection of the oscillator to the receiving sub-system, realized by a quarter-wavelength microstrip coupler, are represented in Fig. 9. The resulting system performance is presented in Figs. 10 in terms of measured voltage across the demodulator output (R_{LOAD} in Fig. 3) versus time: two different respiratory tests have been recorded for an individual performing normal breath (Fig. 10 (a)) and fast breath activity, emulating tachypnea condition (Fig. 10 (b)).

These plots clearly show that the proposed on-board passive demodulator is able to fully distinguish the two respiratory activities under test: in particular, 15 breaths/min (respiratory rate: 0.25 Hz) and 42 breaths/min (0.7 Hz) are detected, respectively. Indeed, the voltage-doubler used as an FM-to-AM demodulator allows to retrieving minima and maxima DC voltage peaks on R_{LOAD} in correspondence of every inspiration and expiration.

It has to be noticed that the oscillator output signal can vary significantly depending on the position of the sensor with respect to the user’s chest; however, it can be noticed that slighter amplitude variations are detected for fast breath, consistently with the fact that this respiratory condition implies smaller chest displacements.

Finally, the energy harvesting performance of the same circuit have been predicted, tested, and reported in Fig. 11. It is worth noticing that for an input power (P_{IN}) equal to 10 dBm, the measured voltage-doubler power conversion PCE

is about 36%, whereas it results to be 20% with 0 dBm of input power.

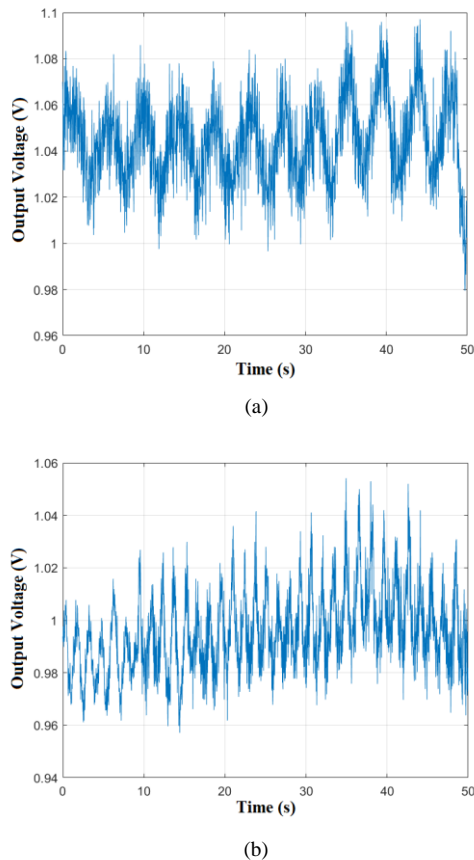


Fig. 10. Output voltage waveforms of the demodulator circuit, for a 50-second test performed with breath rate of (a) 0.25 Hz (15 breaths/min) and (b) 0.7 Hz (42 breaths/min).

The above-mentioned values of PCEs are lower than the ones reported in the literature because, in this case, the matching network is missing, differently from standard energy harvester designs. This is a necessary condition, observed during transient analyses, to properly detect the peaks in correspondence of every inhalation. Concerning the discrepancy between simulated and measured efficiencies, the behavior is very similar, although measurements overestimate simulations: this may be due to the adopted diode model, including the package parasitics (capacitance and inductance), that does not perfectly match the real-life diode behavior at the frequency of 5.8 GHz.

Downstream of the rectifier, a MCU can be adopted in order to elaborate the incoming data; in particular, it has to register the peaks corresponding to a single breathing act and calculate the instantaneous respiratory rate. Then, the MCU has to be also coupled with a transceiver allowing communication through the most common protocols, such as LoRa, Bluetooth Low Energy, ZigBee, etc.

The DC power levels reached at the rectifier output (36 mW and 200 μ W for an input power of 10 dBm and 0 dBm, respectively) would both be able to satisfy the energy requirements of a low-power commercial board including a

microcontroller unit and a transceiver to be employed without the need of a dedicated battery. In particular, accounting for the Semtech SX1280 transceiver adopted for

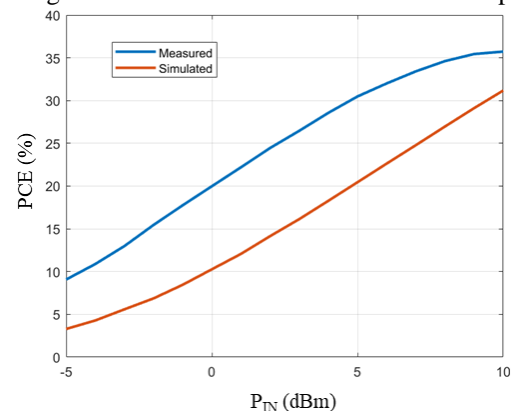


Fig. 11. Simulated and measured percentage PCEs are shown for the voltage-doubler rectifying circuit.

LoRa applications [28] and the PCE reached in this work, it is possible to draw an energy budget estimation for the digital circuitry.

In that sense, considering the incoming power at the rectifier equal to 0 dBm and the efficiency of a commercial power management unit (PMU) to 50%, only 8.68 seconds are necessary to store sufficient energy to sustain the processing operations of the MCU (400 samples per second) and the transmission of information about breathing activity.

Finally, an evaluation of the trade-off between power consumption and data transmission has to be made. The instantaneous transmission of breath rate is feasible, but this is also the most power-consuming scenario. Instead, the selection of two thresholds below and above limit values that can be considered risky would be the best solution to raise an alarm just in case of the presence of dangerous situations.

IV. CONCLUSION

In this work, a wearable sensor exploiting SIL radar techniques has been developed and tested with the aim of remote monitoring normal and deep breath. Validation measurements on different subjects have been conducted in order to corroborate the operation of the overall system. As a further outcome, a receiving sub-circuit has been combined with the SILO by means of a microstrip line coupled with the oscillator output in a unique sensor, thus creating a fully wearable pocket-size device; for the first time, breath rate and waveform are directly available on-board thanks to the design of a circuit composed of a fully passive peak detector for the retrieval of the signal and energy autonomy purposes.

ACKNOWLEDGMENT

This work was partly funded by the Italian Ministry of Education, University and Research (MIUR) within the

framework of the PRIN 2017 “WPT4WID” (Wireless Power Transfer for Wearable and Implantable Devices) project of national interest.

REFERENCES

- [1] P. J. Soh, G. A. E. Vandenbosch, M. Mercuri, and D. Schreurs, "Wearable Wireless Health Monitoring: Current Developments, Challenges, and Future Trends," in *IEEE Microw. Mag.*, vol. 16, no. 4, pp. 55-70, May 2015.
- [2] G. Paolini, D. Masotti, F. Antoniazzi, T. Salmon Cinotti, and A. Costanzo, "Fall Detection and 3-D Indoor Localization by a Custom RFID Reader Embedded in a Smart e-Health Platform," in *IEEE Trans. Microw. Theory Techn.*, vol. 67, no. 12, pp. 5329-5339, Dec. 2019.
- [3] C. Li, Y. Xiao, and J. Lin, "Experiment and Spectral Analysis of a Low-Power Ka-Band Heartbeat Detector Measuring From Four Sides of a Human Body," in *IEEE Trans. Microw. Theory Techn.*, vol. 54, no. 12, pp. 4464-4471, Dec. 2006.
- [4] C. Li, J. Lin, and Y. Xiao, "Robust Overnight Monitoring of Human Vital Signs by a Non-contact Respiration and Heartbeat Detector," in *Proc. 2006 EMBC*, 2006, pp. 2235-2238.
- [5] M. Mercuri *et al.*, "A Direct Phase-Tracking Doppler Radar Using Wavelet Independent Component Analysis for Non-Contact Respiratory and Heart Rate Monitoring," in *IEEE Trans. Biomed. Circuits Syst.*, vol. 12, no. 3, pp. 632-643, Jun. 2018.
- [6] L. Chioukh, H. Boutayeb, L. Li, L. Yakia, and K. Wu, "Integrated radar systems for precision monitoring of heartbeat and respiratory status," in *Proc. 2009 APMC*, Singapore, pp. 405-408, 2009.
- [7] T. Le, A. Moravec, M. Huerta, M. P. H. Lau, and H. Cao, "Unobtrusive Continuous Monitoring of Fetal Cardiac Electrophysiology in the Home Setting," in *Proc. IEEE SENSORS*, New Delhi, India, 2018, pp. 1-4.
- [8] W. Yang, K. Yang, H. Jiang, Z. Wang, Q. Lin and W. Jia, "Fetal heart rate monitoring system with mobile internet," in *Proc. 2014 IEEE ISCAS*, Melbourne, VIC, Australia, 2014, pp. 443-446.
- [9] Yee Siong Lee, P. N. Pathirana, T. Caelli, and R. Evans, "Doppler radar in respiratory monitoring: Detection and analysis," in *Proc. 2013 ICCAIS*, Nha Trang City, Vietnam, 2013, pp. 224-228.
- [10] X. Yang *et al.*, "Diagnosis of the Hypopnea syndrome in the early stage," in *Neural Comput. & Applic.*, vol. 32, pp. 855-866, Feb. 2020.
- [11] D. A. Berlin, R. M. Gulick, and F. J. Martinez, "Severe Covid-19," in *N. Engl. J. Med.*, vol. 383, no. 25, pp. 2451-2460, Dec. 2020.
- [12] D. J. Miller *et al.*, "Analyzing changes in respiratory rate to predict the risk of COVID-19 infection," in *PLoS ONE*, vol. 15, no. 12, Dec. 2020.
- [13] C. Li, Z. Peng, T. Y. Huang, T. Fan, F. K. Wang, T. S. Horng, J. M. Muñoz-Ferreras, R. Gómez-García, L. Ran, and J. Lin, "A Review on Recent Progress of Portable Short-Range Noncontact Microwave Radar Systems," in *IEEE Trans. Microw. Theory Techn.*, vol. 65, no. 5, pp. 1692-1706, May 2017.
- [14] A. D. Droitcour, O. Boric-Lubecke, and G. T. A. Kovacs, "Signal-to-Noise Ratio in Doppler Radar System for Heart and Respiratory Rate Measurements," in *IEEE Trans. Microw. Theory Techn.*, vol. 57, no. 10, pp. 2498-2507, Oct. 2009.
- [15] G. Wang, C. Gu, T. Inoue, and C. Li, "A Hybrid FMCW-Interferometry Radar for Indoor Precise Positioning and Versatile Life Activity Monitoring," in *IEEE Trans. Microw. Theory Techn.*, vol. 62, no. 11, pp. 2812-2822, Nov. 2014.
- [16] D. Zito *et al.*, "SoC CMOS UWB pulse radar sensor for contactless respiratory rate monitoring," in *IEEE Trans. Biomed. Circuits Syst.*, vol. 5, no. 6, pp. 503-510, Dec. 2011.
- [17] F. K. Wang, C. J. Li, C. H. Hsiao, T. S. Horng, J. Lin, K. C. Peng, J. K. Jau, J. Y. Li, and C. C. Chen, "A Novel Vital-Sign Sensor Based on a Self-Injection-Locked Oscillator," in *IEEE Trans. Microw. Theory Techn.*, vol. 58, no. 12, pp. 4112-4120, Dec. 2010.
- [18] T. S. Horng, "Self-injection-locked radar: an advance in continuous-wave technology for emerging radar systems," in *Proc. 2013 APMC*, Seoul, South Korea, pp. 566-569, 2013.
- [19] F. Wang, Y. Chou, Y. Chiu, and T. Horng, "Chest-Worn Health Monitor Based on a Bistatic Self-Injection-Locked Radar," in *IEEE Trans. Biomed. Eng.*, vol. 62, no. 12, pp. 2931-2940, Dec. 2015.
- [20] R. Kukkapalli, N. Banerjee, R. Robucci, and Y. Kostov, "Micro-radar wearable respiration monitor," in *Proc. 2016 IEEE SENSORS*, Orlando, FL, USA, 2016, pp. 1-3.
- [21] C. Hsu, L. Hwang, F. Wang, and T. Horng, "Wearable Vital Sign Sensor Using a Single-Input Multiple-Output Self-Injection-Locked Oscillator Tag," in *Proc. IEEE MTT-S IMS*, Philadelphia, PA, USA, pp. 248-251, 2018.
- [22] C. Tseng, L. Yu, J. Huang, and C. Chang, "A Wearable Self-Injection-Locked Sensor With Active Integrated Antenna and Differentiator-Based Envelope Detector for Vital-Sign Detection From Chest Wall and Wrist," in *IEEE Trans. Microw. Theory Techn.*, vol. 66, no. 5, pp. 2511-2521, May 2018.
- [23] G. Paolini, M. Feliciani, D. Masotti, and A. Costanzo, "Experimental Study of a Self-Oscillating Antenna at 5.8 GHz for Breath Monitoring," in *Proc. 2019 IEEE-APS APWC*, Granada, Spain, 2019, pp. 198-200.
- [24] G. Paolini, M. Feliciani, D. Masotti, and A. Costanzo, "Toward an Energy-Autonomous Wearable System for Human Breath Detection," in *Proc. 2020 IEEE MTT-S IMBioC*, Toulouse, France, 2020, pp. 1-3.
- [25] A. Costanzo, D. Masotti, N. Arbizzani, V. Rizzoli, and F. Matri, "A microwave sensor system based on reverse modelling of the array factor," in *Proc. 2012 6th EUCAP*, Prague, Czech Republic, pp. 3446-3449, 2012.
- [26] C. Hsu, L. Hwang, F. Wang, and T. Horng, "Wearable Vital Sign Sensor Using a Single-Input Multiple-Output Self-Injection-Locked Oscillator Tag," in *Proc. 2018 IEEE MTT-S IMS*, Philadelphia, PA, USA, pp. 248-251, 2018.
- [27] R. E. Arif, W. C. Su, M. C. Tang, T. S. Horng, and F. K. Wang, "Chest-worn self-injection-locked oscillator tag for monitoring heart rate variability," in *Proc. 2020 IEEE MTT-S IMS*, Los Angeles, CA, USA, pp. 512-515, 2020.
- [28] G. Paolini, M. Guermandi, D. Masotti, M. Shanawani, F. Benassi, L. Benini, and A. Costanzo, "RF-Powered Low-Energy Sensor Nodes for Predictive Maintenance in Electromagnetically Harsh Industrial Environments," *Sensors*, vol. 21, no. 2, pp. 386-403, Jan. 2021.



Giacomo Paolini (GS'18-M'21) received the M.Sc. degree in biomedical engineering and the Ph.D. degree in electronics, telecommunications, and information technologies engineering from the University of Bologna, Bologna, Italy, in 2016 and 2021, respectively. He joined the Interdepartmental Center for Industrial ICT Research (CIRI ICT), University of Bologna, as a Research Fellow within the EU-supported "HABITAT" project in 2016. He is currently working as a

Post-Doctoral Researcher at the Department of Electrical, Electronic and Information Engineering "G. Marconi" (DEI), University of Bologna. His research interests include microwave radar systems for biomedical applications, indoor positioning exploiting RFID technologies, and far-field wireless power transfer systems.



Mazen Shanawani received the M.Sc. degree in communication systems and signal processing from the University of Bristol, Bristol, U.K., and the Ph.D. in electronics, telecommunications, and information technologies engineering from the University of Bologna, Bologna, Italy. In 2020, he joined the University of Bologna as a Junior Assistant Professor to participate to the teaching and research activities relevant to wireless power transfer. He has authored several articles and conference proceedings, a

co-author of the Wireless Power Transmission for Sustainable Electronics COST WiPe – IC1301 book, reviewer in Nature Communications open access besides many other journals, a prize winner of the Lions Club Bologna for scientific research and technological innovation in 2020, and a Ph.D. scholarship winner. His research interests include co-simulation and optimization of linear and nonlinear energy transmitters and harvesters,

energy-efficient antenna arrays, efficient electromagnetic modelling techniques and modelling of tunnelling devices.



Diego Masotti (M'00–SM'16) received the Ph.D. degree in electric engineering from the University of Bologna, Italy, in 1997. In 1998 he joined the University of Bologna and is now Associate Professor of electromagnetic fields. His research interests are in the areas of nonlinear microwave circuit simulation and design, with emphasis on nonlinear/electromagnetic co-design of integrated radiating subsystems/systems for wireless power transfer and energy harvesting applications. He authored more than 70 scientific publications on peer reviewed international journals and more than 130 scientific publications on proceedings of international conferences. Dr. Masotti serves in the Editorial Board of the International Journal of Antennas and Propagation, the Journal of Wireless Power Transfer, IEEE Access, and Electronics Letters and is a member of the Paper Review Board of the main Journals of the microwave sector.



Dominique M. M.-P. Schreurs (S'90–M'97–SM'02–F'12) received the M.Sc. degree in electronic engineering and the Ph.D. degree from the University of Leuven (KU Leuven), Leuven, Belgium, in 1992 and 1997, respectively. She has been a Visiting Scientist with Agilent Technologies, Santa Rosa, CA, USA, ETH Zürich, Zürich, Switzerland, and the National Institute of Standards and Technology, Boulder, CO, USA. She is currently a Full Professor with KU Leuven, where she is also the Chair of the Leuven ICT

(the Leuven Centre on Information and Communication Technology). Her current research interests include the microwave and millimeter-wave characterization and modeling of transistors, nonlinear circuits, and bioliquids, and system design for wireless communications and biomedical applications. Prof. Schreurs served as the President of the IEEE Microwave Theory and Techniques Society from 2018 to 2019. She was an IEEE MTT-S Distinguished Microwave Lecturer. She has also served as the General Chair for the Spring Automatic RF Techniques Group (ARFTG) conferences in 2007, 2012, and 2018, and the President of the ARFTG organization from 2018 to 2019. She was the Editor-in-Chief of the IEEE Transactions on Microwave Theory and Techniques.



Alessandra Costanzo (A'99–M'02–SM'13) is currently a Full Professor with the Alma Mater Studiorum, University of Bologna, Cesena, Italy. She has authored more than 260 scientific publications in peer-reviewed international journals and conferences and several chapter books. Recently, she has proposed novel solutions for energy-autonomous RF systems based on the wireless power transmission, adopting both far-field and near-field solutions, for several power

levels and operating frequencies. Her current research interests include CAD algorithms for multi-domain co-design and modeling of active nonlinear microwave/RF circuits. Dr. Costanzo is a member of the MTT-24 Committee on Radio Frequency Identification (RFID). She is the Past-Chair of the MTT-26 Committee on Wireless Energy Transfer and Conversion and has been the TPC Co-Chair of MTT-S WPTC2019. Since 2016, she has been the Steering Committee Chair of the IEEE Journal of Radio Frequency Identification. She is past Associate Editor for the IEEE Transactions on Microwave Theory and Techniques, associate editor of the Cambridge International Journal of Microwave and Wireless Technologies. She is a co-founder of the EU COST Action IC1301 WiPE Wireless Power Transfer for Sustainable Electronics. She is the MTT-S Representative and a Distinguished Lecturer of the Council on Radio Frequency Identification (CRFID). In November 2021 she has been

elevated to IEEE Fellow, effective January 2022 with the following citation: “for contributions to nonlinear electromagnetic co-design of RF and microwave circuits”.